

## Application of an Advanced Variance Reduction Technique for Bulk Shield Calculations of the IFMIF-DONES facility

Yuefeng Qiu, Stanislav Simakov, Ulrich Fischer

Karlsruhe Institute of Technology, Hermann-von-Helmholtz-Platz 1, 76344 Eggenstein-Leopoldshafen, Germany  
yuefeng.qiu@kit.edu

**Abstract** – The advanced variance reduction technique provided by the ADVANTG code has been applied for bulk shield calculations of the IFMIF-DONES (International Fusion Material Irradiation Facility- DEMO Oriented NEutron Source) facility. Compared to a normal Monte Carlo run, 5 times more mesh cells with non-zero tracking results are obtained by using the ADVANTG generated weight-window (WW) mesh. The computational speed, however, is 260 times slower, and the statistical error is high. A program has been developed to tune the WW distributions in order to mitigate this problem. The tuned ADVANTG WW mesh shows a speed-up by a factor 37 compared to the no-tuned case, and also achieves further improvement of the tracking results. In addition, the source subroutine of McDeLicious has been extended to produce constant-weight source neutrons. Its impact on the computational speed and the numerical results used together with the WW mesh has been also assessed.

### I. INTRODUCTION

IFMIF-DONES (International Fusion Material Irradiation Facility- DEMO Oriented NEutron Source, brief as DONES) [1, 2] is a downgraded IFMIF-based neutron irradiation facility which aims at providing the irradiation data required for the construction of a DEMO fusion power plant. This facility produces intense neutrons with a neutron flux up to  $10^{14}$  n/cm<sup>2</sup>/s and energy up to 55 MeV. The shielding of the facility is a very important issue in the test cell (TC) design. The heavy concrete bioshield of the TC, housing the irradiation test modules, is up to 4 m thick. The biological dose rate distribution outside the bioshield needs to be known with sufficient accuracy for assessing the accessibility during operation and maintenance periods of the facility.

The computational assessment of the radiation penetrating the thick bioshield is, however, a great challenge for transport simulations. This applies in particular for the Monte Carlo (MC) particle transport technique as available with codes like MCNP5 [3]. Sophisticated variance reduction techniques are required to obtain a sufficient good statistics for the responses scored behind the massive bulk shield. Applying advanced weight-window (WW) mesh generation tools such as ADVANTG [4] could have potential benefits over the standard approach using e. g. MCNP's WW generator algorithm. The ADVANTG code solves the Boltzmann transport equation using deterministic methods, and then generates WW using the calculated neutron/gamma flux. However, neutron streaming in channels such as beam ducts would be an issue for deterministic codes. In this work, the application of ADVANTG to generate WW for reducing the variance of DONES MC simulation has been evaluated.

### II. COMPUTATION MODEL AND METHODOLOGY

#### 1. Computation geometry

The MCNP geometry of the DONES TC is shown in Fig. 1. It includes the target and the bioshield. The bioshield made of heavy concrete has a 2 ~ 4 m in thickness in different directions. There also two beam ducts with an average cross-section of 80 × 200 mm, pointing to the target where the high energy neutrons are generated. There is no material in the beam duct. Therefore the neutrons streaming from the target are very strong along the beam ducts.

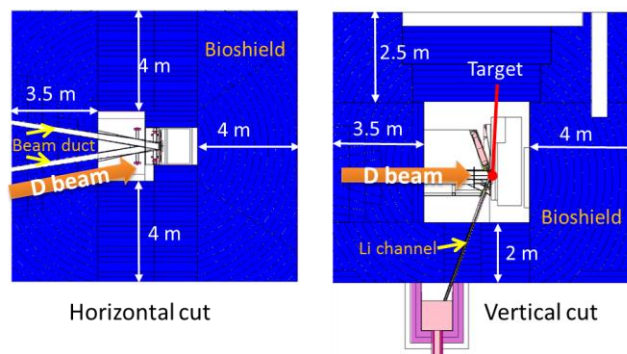


Fig. 1. Geometry of the DONES TC in horizontal cut-view at the beam level and vertical cut-view at target center.

#### 2. Source modeling

The neutron source setup is implemented as source subroutine of MCNP5, i.e. McDeLicious [5], and utilizes external cross-section data files for the simulation of the interaction of deuterons and lithium nuclei. McDeLicious samples the deuterium particles from a two-dimensional beam profile, and generates neutrons from the simulation of deuterium particles interacting with the lithium target. In this subroutine, the number of deuterium particles is used for normalization. This means that each deuterium particle produces one neutron. Therefore this neutron is assigned a

different weight according to the probability for the generation of D-Li source neutrons given by the neutron yields as function of deuteron energy. However, ADVANTG uses the MCNP source definition card SDEF and converts it into a discretized source specification. The user defined source subroutine adopted in McDeLicious does not allow the direct application of ADVANTG to DONES.

A trade-off solution has been adopted in this work using a dedicated SDEF representation to approximate the D-Li source generation modelled in the McDeLicious source subroutine. First the neutron energy and angular distributions were calculated using a slab-shaped envelope as shown in Fig. 2. This envelope covers the target area where the deuterium-lithium reactions take place. It is perpendicular to the beam direction ( $9^\circ$  angle to the X direction) on its front and rear surface. The extensions of the envelope on the other four sides are quasi-infinite, making it reasonable to tally the neutron angular distribution on the front and rear surface using the MCNP surface current tally F1. This envelope is void, and the neutrons escaping from the envelope are killed. The neutron energy spectrum obtained inside the envelope reproduces the McDeLicious neutron spectrum. The neutron flux is sampled in a 211 VITAMIN-J+ group structure, and is normalized by the total neutron flux to obtain the probability density function. The angular distribution of neutron currents going through the front and rear surface are tallied with 18 intervals of angle cosine from -1 to 1. The results are normalized to the total current in order to obtain the angular probability density function. The calculated energy and angular probability density functions are used for modeling the SDEF source in MCNP. Fig. 3 shows the energy probability per lethargy, and angular probability per solid angle.

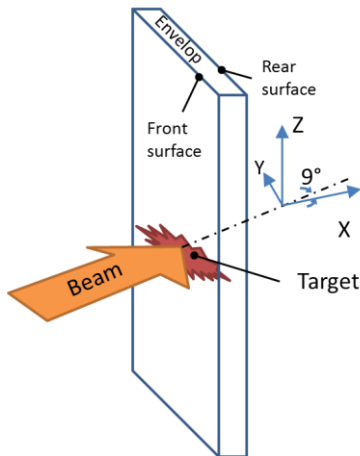
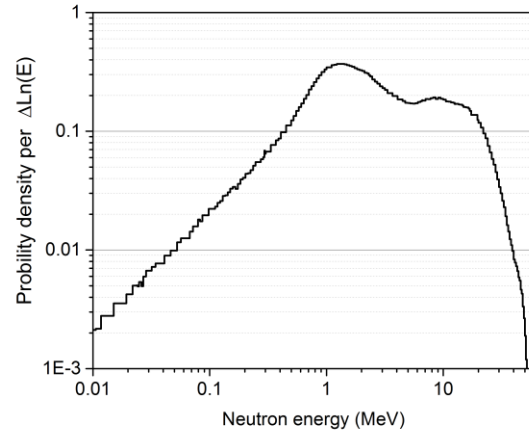
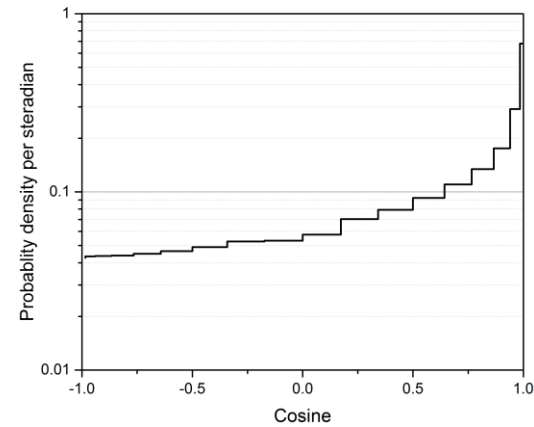


Fig. 2. Quasi-infinite slab-shaped envelope used for obtaining the neutron source energy and angular distribution. The slab is perpendicular to the beam direction ( $9^\circ$  to the X direction) and covers the Li target area.



(a) Energy probability density per lethargy.



(b) Angular probability per steradian.

Fig. 3. Neutron energy and angular distribution sampled using the envelope shown in Fig. 2.

Then, a MCNP SDEF card has been created covering a box region with size of  $3 \times 20 \times 5$  cm in X, Y, Z direction. It is located at the Li target area where the deuterium-lithium reaction takes place. The source neutrons are sampled homogeneously inside this volume. The reference vector of angular distribution is set parallel to the beam direction ( $9^\circ$  angle to the X direction). Although this SDEF source card is able to approximate the angular and energy distributions of source neutrons, the distribution of the neutron weight cannot be correctly reproduced because the SDEF card supports only a constant weight value. The weight distribution of source neutron produced by McDeLicious is sampled using  $10^5$  source neutron as shown in Fig. 4. The probability-weighted mean value of the weight value is 0.085, hence this weight value is used for the SDEF representation. Theoretically, the physics of the simulation is not affected by using the WW generated with a constant weight. The source neutrons with weight value outside the

WW will be either possibly split if the weight is higher than the upper bound, or possibly killed if the weight is lower than the lower bound. However, the influence on actual simulation results remains to be studied.

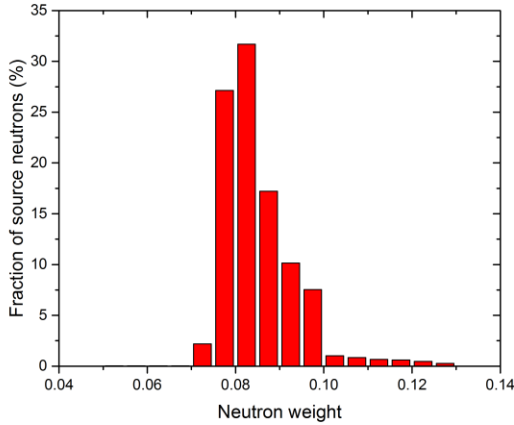


Fig. 4. Weight distribution of source neutrons produced by the McDeLicious simulation.

### III. VARIANCE REDUCTION ASSESSMENT

#### 1. Calculation setups

The purpose of this assessment is to investigate the applicability of the ADVANTG code to DONES shielding calculation. Therefore, the variance reduction efficiency (especially in the bioshield), tally results accuracy, as well as the computational efficiency after employing the ADVANTG WW mesh are evaluated by comparisons with normal MCNP runs. Three calculation cases have been performed — The first case (abbreviated as Case-Ref) is a MCNP run without any WW mesh; The second case (called Case-McWW) is a MCNP run with a WW mesh generated for cell-based tallies using the MCNP code; The third case (Case-Adv) is a MCNP run with ADVANTG generated WW mesh for a neutron mesh tally covering the whole DONES TC model.

The Case-Ref is considered as the reference case, which provides references for the comparisons of computational speed and result accuracy among the cases. A mesh tally with resolutions of  $10 \times 20 \times 10$  cm ( $117 \times 55 \times 120$  intervals) in X, Y, Z direction is used for tallying the neutron flux in the whole TC. The average neutron flux spectrum in a region behind the High Flux Test Module (HFTM), as indicated in Fig.5, is tallied with a 211 group Vitamin-J+ energy intervals. Six cell-based flux tallies (MCNP F4 cards) are assigned for the cells at the different sides of the bioshield. In addition, the number of particle histories (NPS) per minute of computation time (CTM) (calculated by the wall clock time multiplied by the number of processors) used was collected after a simulation of  $10^8$

NPS to compare the computational speed. Only neutrons are simulated, and the neutron cross-section library FENDL-3.1b [6] was used.

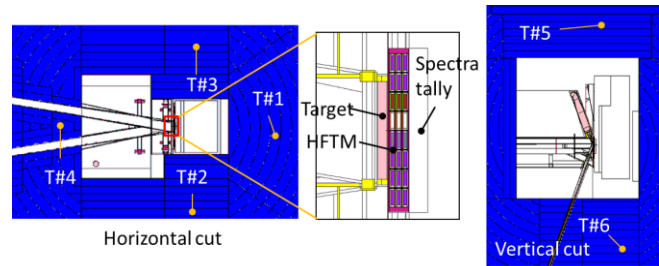


Fig. 5 Tally locations in the TC model.

In the Case-McWW, a WW mesh with  $50 \times 49 \times 48$  intervals in X, Y, Z directions and 4 energy groups ( $10^{-4}$ , 0.01, 1, 100 MeV) was generated by an independent MCNP run, aiming at achieving good statistics in the six cell-based tallies indicated in Fig. 5. Then another MCNP run was made to calculate the results using the WW mesh.

In the Case-Adv, a WW mesh was generated by the ADVANTG code, using directly the MCNP input file for the geometry modeling and also the material assignment. The source definition of this MCNP input uses the SDEF card described in Section II.2. A rectilinear mesh configuration has been set up, which has  $120 \times 80 \times 125$  intervals in X, Y and Z direction. In this mesh, fine resolutions up to  $10 \times 3 \times 2$  cm are assigned for the region of the target assembly and the HFTM, as well as the beam duct and the Li channel in order to calculate more accurately the streaming neutron flux. In other regions a normal resolution of  $20 \times 20 \times 20$  cm is used to control the size of WW mesh file. The general purpose shielding library 27n19g provided with the ADVANTG code was adopted, which has 27 neutron groups. The FW-CADIS method with the global weighting treatment, which is suitable for generating WW for mesh tallies, was adopted with 5 order of the Legendre scattering-angle expansion. The parallel computation mode has been turned on to enable the use of 128 processors ( $8 \times 16$  blocks in X and Y mesh direction) in the transport calculation phase.

#### 2. Result comparisons

The calculation of the Case-Ref and Case-McWW are finished normally with  $10^8$  NPS. However, in the Case-Adv only a  $10^7$  NPS can be finished due to the extremely slow computational speed. As shown in the Table 1, the ration NPS/CTM of Case-Adv is around 260 times smaller than the Case-Ref, while The NPS/CTM of Case-McWW is comparative with the Case-Ref. Although a coarse WW mesh and less energy groups were used in the Case-McWW, the slow-down of computational speed is huge in Case-Adv and makes the use of ADVANTG WW impractical.

Horizontal cut views of the neutron flux mesh tallies are shown in Fig.6, which provides useful information for understanding the problem of Case-Adv. In the Case-Ref, results can be obtained within 1.5~2 m of the bioshield, but only 1~1.5 m of them have good enough statistics (considering statistical error below 10%). The Case-McWW has slightly better statistics in beam downstream bioshield (right side seeing from Fig. 6(b)), but worse statistics on the other sides comparing to the Case-Ref case. Since the MCNP WW generator can optimize cell-based or surface-based tallies (e.g. volume flux tally F4), but not superimposed mesh tallies, obtaining a WW mesh for the whole TC model requires much more efforts than using ADVANTG. These efforts include not only the tuning on the targeting tallies, but also several iterations of MCNP runs to extend the covering regions of particle tracks. These are major inefficiencies of the MCNP WW mesh generation approach. For the Case-Adv in Fig.6(c), large areas are covered with particle tracks. The statistics is good (<10%) in the beam downstream region, as well as the beam duct surrounding region. However, the statistics on the target lateral side (upper and lower side seeing from Fig. 6(c)) are still poor. It is computational expensive to increase the NPS for Case-Adv, and the statistics in these poor region will very like be enhanced much slower than the beam downstream and beam duct surrounding region. It is suspected that the WW in some regions, e.g. beam duct surroundings, are excessive low, which results in over-splitting of particle tracks. These particle histories, called *long histories*, usually consumes very long computation time in a single processor, and cause other processors to wait before one result collection.

Fig. 7 presents the relation of fraction of mesh cells and statistical errors. According to the MCNP manual [3], results with statistical error above 50% must be considered garbage; results with errors between 20 and 50% may be off by a factor of few; results with errors between 10% and 20% might be still questionable; while results with statistical error less than 10% are considered reliable. Case-Ref provides statistically reliable results for 7% of the mesh cells, Case-McWW for 4%. and Case-Adv for 6%. The number of cells with statistical error large than 10% significantly increases for the Case-Adv.

Fig. 8 shows the neutron flux spectra in the tally region behind the HFTM as indicated in Fig. 5, as well as the ratio taken the Case-Ref as reference. Good agreements are found between Case-McWW and Case-Ref. However, the deviation between Case-Adv and Case-Ref are not small, especially in the energy range < 0.1 MeV. It is likely due to the high statistical error of the results of Case-Adv (more than 20% of statistical error in results <0.01 MeV). However, the Case-Adv has better statistics in the bioshield, when seeing from Fig. 9 which provides the volume integrated neutron flux in cell-based tallies of the bioshield. Very good agreements between Case-Adv and Case-Ref are obtained, as well as good statistics. The Case-McWW, on

the other hand, has fare agreement in some tallies, e.g. T#3, but basically within statistical error.

	WW generation time (CTM)	Computation speed (NPS/ CTM)
Case-Ref	--	13999
Case-McWW	6562.37	12401
Case-Adv	1715.2	54

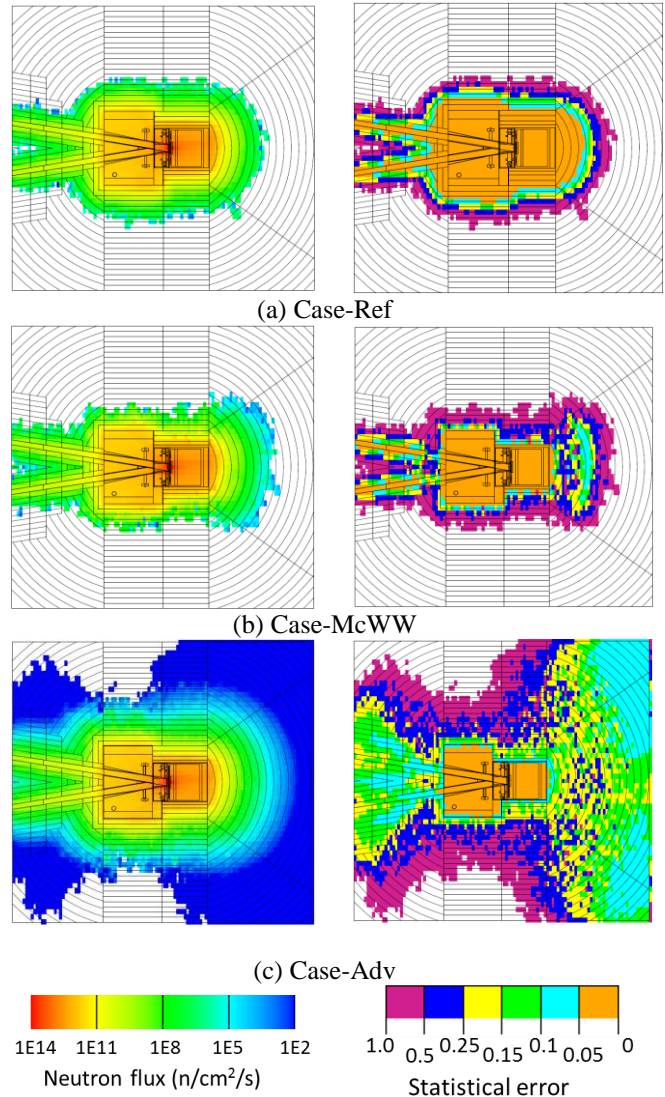


Fig. 6 Neutron flux (left) and statistical error (right) of the horizontal cut-view at the beam level.

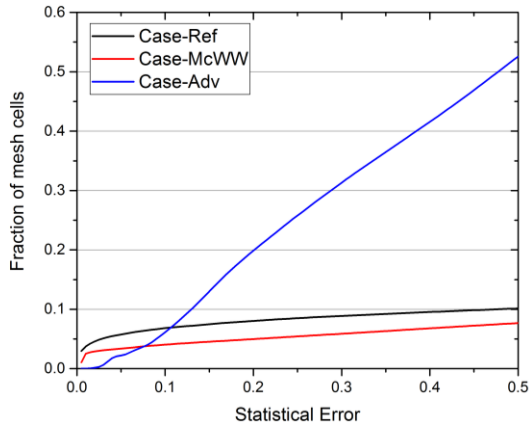


Fig. 7 Plot of the fraction of cells with statistical error less than the corresponding statistical error.

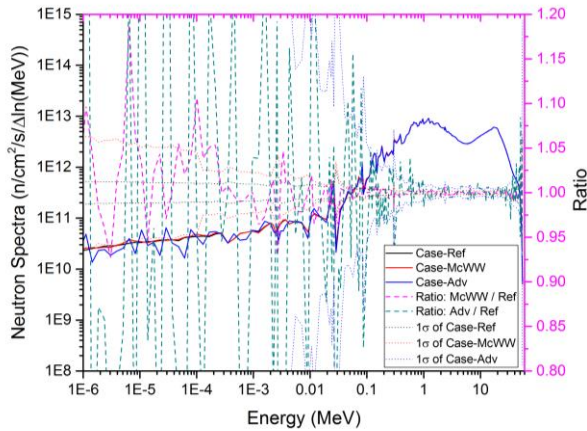


Fig. 8 Neutron flux spectra (the vertical axis on the left) behind the HFTM at the position marked as “spectra tally” in Fig. 5. The results of Case-Ref are taken as reference in calculating the ratios (the vertical axis on the right). 1 $\sigma$  indicates the value of  $1 \pm$  statistical error using the vertical axis on the right.

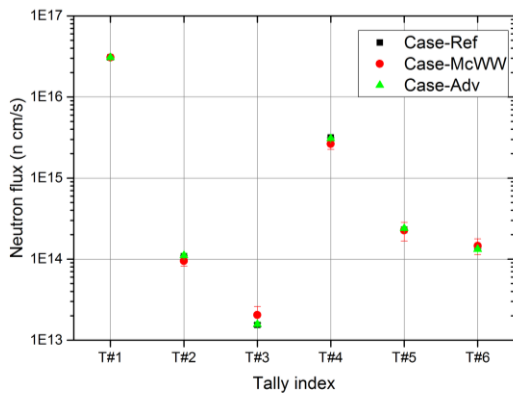


Fig. 9 Cell-based neutron flux tallies of cell inside the bioshield at six locations given in Fig. 5. Neutron flux over the cell volume (n cm/s) is presented.

## IV. ADVANTG WW OPTIMIZATION

As discussed above, the ADVANTG generated WW mesh has positive effect in achieving better statistics in the bioshield, whereas the computational speed is significantly slow when employing the WW mesh. In this work, a further adjustment of the ADVANTG WW has been achieved by developing a WW tuning program. In addition, the impact of the constant source neutron weight has been assessed by extending the McDeLicious code.

### 1. WW tuning program

For studying the reason of the slow computational speed in Case-Adv, the 7<sup>th</sup> group (0.015~0.11 MeV) of the WW lower bound was extracted from the ADVANTG WW file and shown in the Fig. 10. Although each WW has a lower bound and an upper bound, the WW upper bound is always 5 times of the lower bound which is set as a parameter in the MCNP input file. Therefore, the lower bound weight distribution reveals the WW distribution. According to the ADVANTG WW generation algorithm, the weight is inversely proportional to the flux value, since a mesh tally covering the whole TC geometry is targeted for variance reduction. From Fig. 10 it is found that the weight value change  $\sim 10^{-8}$  along the beam ducts, whereas the change of the neutron flux is around 0.01~0.001 by observing Fig. 6(a). Fig. 6(a) also shows that the neutron flux surrounding the beam duct is within the same order of magnitude along the beam duct, while this trend is not revealed in the WW distribution. In this situation, a high-weight neutron back-scattered from the target into the beam duct will be reduced million times on its weight, but in the meantime it will be split into millions of neutrons, which cause the neutron history extremely long. On the other hand, the statistics along the beam duct are excessively good (as shown in the Fig. 6(c)), especially at the entry of the beam duct (left side of the duct). Long histories are also found in the beam downstream bioshield, by observing the excessive good statistics in Fig. 6(c) for this location.

In order to mitigate the long-history problem, a python program has been developed to process the WW mesh and tuning the WW value. The WW mesh import and export interfaces has been developed based on the PyNE tool-suites [7], extracted and modified to become a python module independent from PyNE. The interface is able to process both neutron and photon WW in a rectilinear mesh. This program provides two methods to define a container and extract the cells from the rectilinear mesh (here called global mesh) — extracting a block of cells in the global mesh by defining a starting point and dimensions along X, Y, Z directions (Method-1); or extracting the cells inside a “tunnel” with a box or cylinder shape (Method-2).

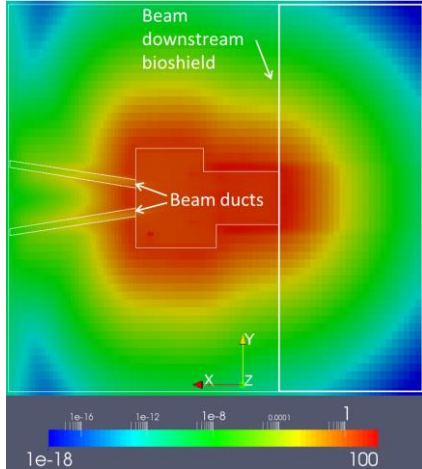


Fig. 10 Distribution of the WW lower bound generated by ADVANTG. The 7<sup>th</sup> neutron energy group is chosen here for illustration.

Fig. 11 uses the 2D figure to illustrate the 3D case. It is straight-forward to extract the cells using Method-1, since the center points of cells is easy to be checked whether they are inside the global container. If Method-2 is used, the length and cross-section dimension of the tunnel, as well as the local coordinate vector, have to be provided. In order to detect the global cells inside the tunnel, a structured mesh with uniform intervals in each local coordinate direction (X'-Y') is generated, and the nodes of this local mesh are then transformed into the global coordinate (X-Y). The mesh nodes in a cylinder tunnel have to be first transformed from the local cylindrical coordinate to the local Cartesian coordinate, and then to the global (Cartesian) coordinate. The global mesh cells which contain the local mesh nodes are detected and extracted. The resolutions of the local mesh should be finer (factor of 1.5~2 suggested) than the resolutions of the global mesh, so that some contained cells are not missing. A sweep direction has to be defined for tuning the WW value. The container plane which is perpendicular to the sweep direction is considered as reference plane (as indicated in Fig. 11), and the first sweep block paralleling to the reference plane is called reference block. Consider the sweep distance along the container as the unit distance, a relative distance  $\delta$  ( $0 \leq \delta \leq 1$ ) is calculated between the center of the global cell and the reference plane. Using a global factor  $\lambda$ , the new WW value  $W_i'$  of cell  $i$  value can be linearly or exponentially tuned by multiplying a factor to its previous value  $W_i$ :

$$W_i' = W_i \lambda \delta \quad ,$$

$$\text{or } W_i' = W_i \exp(\lambda \delta) \quad , \quad (1)$$

or multiplying a factor to the value of the reference block  $W_0$ :

$$W_i' = W_0 \lambda \delta$$

$$\text{or } W_i' = W_0 \exp(\lambda \delta) \quad . \quad (2)$$

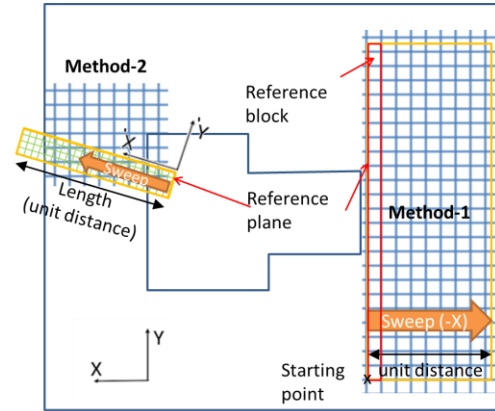


Fig. 11 Illustration of the mesh extraction and WW tuning methods used in the WW tuning program.

A new WW mesh was accordingly produced as shown in Fig. 12, which takes again the 7<sup>th</sup> group for illustration. The WW in the indicated blocks and beam ducts are tuned. Method-1 was used for Block-1 and Block-2, and Method-2 is used for two beam ducts. Block-1 covers the whole model in Z direction, and is swept along +X direction using the method given in Eq.1 with  $\lambda = 6.9$  (around factor of 1000 in the ending sweep block). Block-2 covers the beam duct region and, 2 m above and below beam leave in Z direction, and is swept along -X direction using also the method given in Eq.1 with  $\lambda = 11.5$  (around factor of  $10^5$  in the ending sweep block). In addition, two beam ducts are sweep from inner TC to beam entry (right to left side see from Fig. 12) using the method given in Eq. 2 with  $\lambda = -6.9$  (around factor of  $10^{-3}$  decrease at the beam entry).

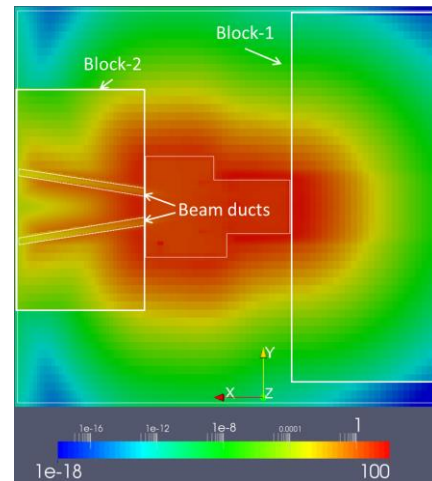


Fig.12 Distribution of the ADVANTG WW lower bound after tuning the indicated regions. The 7<sup>th</sup> neutron energy group is chosen here for illustration.

## 2. Source neutron with constant weight

Because the source neutrons produced by McDeLicious have different weights, there are always warning messages given by MCNP on the source neutron weight above or below WW bounds. The impact of using a WW mesh with non-constant source particle weight on the variance reduction effect, as well as the simulation results, has to be assessed. The McDeLicious code therefore has been extended in this work to enable the simulation of source neutrons generated with constant weight.

The targeted constant weight  $\omega_0$  has to be higher than most of the possible neutron weights. Using the Russian roulette technique, a neutron with weight  $\omega$  will be killed if  $\omega < \xi\omega_0$ , where  $\xi$  is a random number and  $0 < \xi < 1$ . If the neutron is killed, the source neutron will be resampled, but the neutron history is not terminated. If the neutron survives from the random game, this neutron will be assigned a new weight of  $\omega_0$ . The amount of neutrons killed, denoted as  $N_{kill}$ , is recorded along the simulation. Denoting the NPS as  $N_{nps}$ , the results produced by MCNP should be multiplied with a factor

$$\lambda = 1 - \frac{N_{kill}}{N_{kill} + N_{nps}}. \quad (3)$$

## 3. Results and discussions

The WW produced in the Case-Adv was tuned using the methods and parameters discussed in Section IV.1 (denoted as Case-Tuned). A new ADVANTG run was conducted to produce another WW mesh with target weight value of 0.130. This new WW mesh was similarly tuned as Case-Tuned using the same setup (called Case-ConstW). A consistent simulation setup as in Section III.1 was used. The newly extended McDeLicious code was used to calculate the Case-ConstW, and the results were renormalized with a factor of 0.695 calculated using Eq.3.  $10^8$  particle histories were finished in both cases, and the computational time is shown in Table 2. It is found that a remarkable speed-up is achieved using the tuned WW mesh. Although the computational speed is still 7 times slower than the Case-Ref, the Case-Tuned is 37 times faster than the Case-Adv. The Case-ConstW shows almost the same computational speed as Case-Tuned, which implies that the use of WW with different source neutron weights does not clearly slow down the computational speed.

Fig. 13 presents the neutron flux results and statistics of these two cases. Fig. 13(a) shows that the Case-Tuned produces results for larger area compared to the Case-Adv in Fig.6 (c). The excessively good statistics around the beam ducts and beam downstream area are controlled, which implies the long history is mitigated. Fig.14 presents the relation of fraction of mesh cells and statistical errors

plotted similar as in Fig. 7. The Case-Tuned and Case-ConstW produce results in more than 70% of the mesh cells. The amount of cells with good statistical results is at a similar level as in Case-Ref, which is 7%. Since the long-history problem is mitigated, the statistics can be further improved by increasing NPS. Also the WW in the poor statistics region is possible to be further optimized using the WW tuning program, so that the particle tracks will be increased to enhance the statistics.

Table 2. Computational speed comparison.

	Computation speed (NPS/ CTM)
Case-Tuned	2024
Case-ConstW	2054

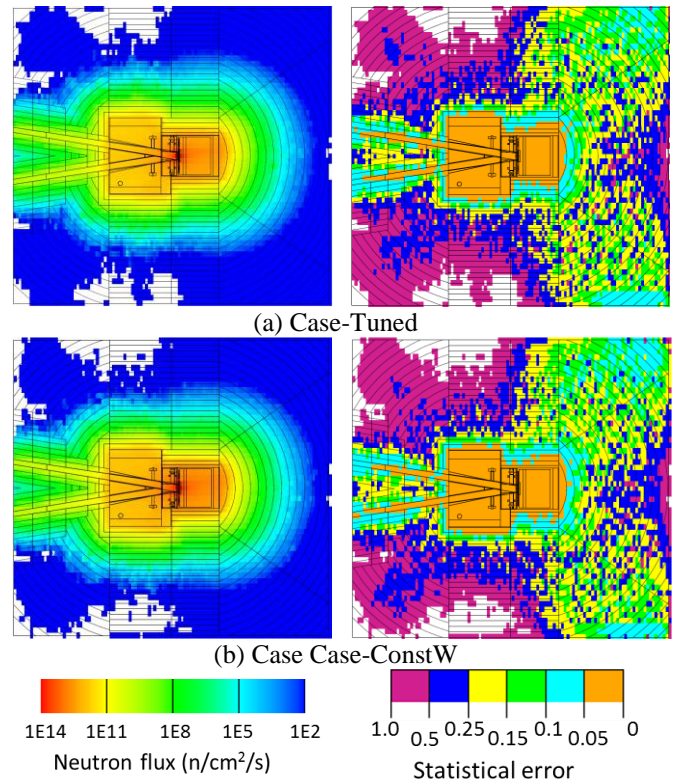


Fig. 13 Neutron flux (left) and statistical error (right) of the horizontal cut-view at the beam level.

Fig. 15 shows the cell-based tally results in six located inside the bioshield. All of the results agree very well among Case-Ref, Case-Tuned and Case-ConstW. Fig. 16 shows again the neutron flux spectra as well as the ratio. The deviations of Case-Tuned and Case-ConstW from the Case-Ref have very similar behaviors, and are related very likely to the statistical errors. A possible reason is that, the WW generated in this work by ADVANTG is aimed at reducing the variance of the total flux. Therefore, the WW is optimized by ADVANTG so that energy groups with higher neutron flux have better statistics than those with lower flux.

The comparison between the Case-Tuned and Case-ConstW does not provide any valuable findings, which indicates that the use of McDeLicious with WW mesh does not clearly affect the simulation results.

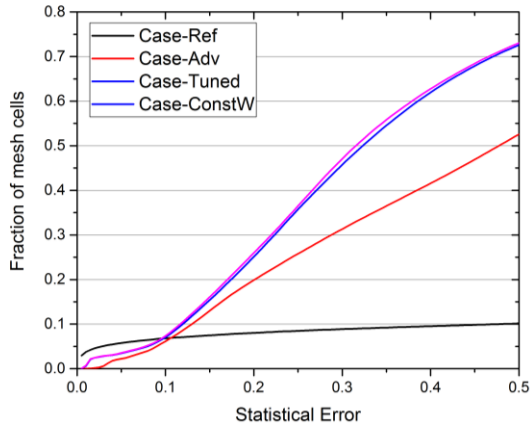


Fig. 14 Plot of the fraction of cells with statistical error less than the corresponding statistical error.

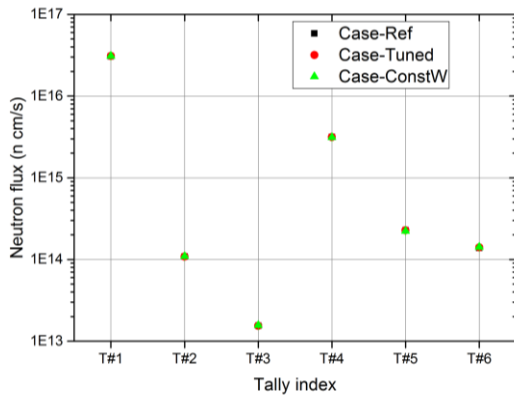


Fig. 15 Cell-based neutron flux tallies of cells inside the bioshield at six locations given in Fig. 5. The neutron flux integrated over the cell volume (n cm/s) is presented.

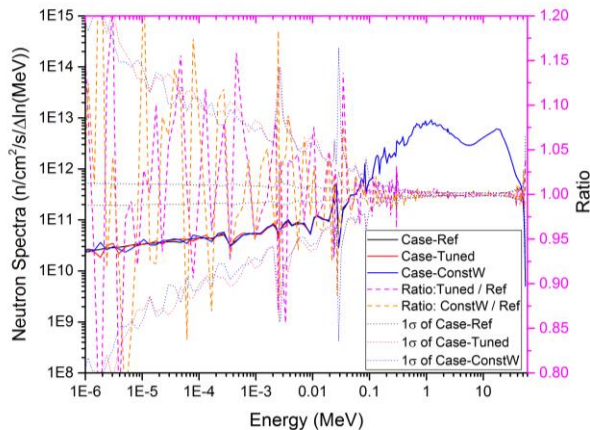


Fig. 16 Neutron flux spectra (the vertical axis on the left) behind the HFTM at the position marked as “spectra tally”

in Fig. 5. The results of Case-Ref are taken as reference in calculating the ratios (the vertical axis on the right).  $1\sigma$  indicates the value of  $1 \pm$  statistical error using the vertical axis on the right.

#### IV. CONCLUSIONS

The effect of using an ADVANTG generated WW mesh to reduce the variance in Monte Carlo shielding calculations has been evaluated for the DONES TC. A MCNP SDEF source has been modeled based on the source neutron spectra, angular distribution and weight distribution produced by the McDeLicious code, in order to enable the WW mesh generation in ADVANTG code. The comparison with two normal MCNP runs, without and with WW generated by MCNP, shows that the MCNP run with the ADVANTG WW mesh is able to produce more than 5 times more mesh cells with non-zero tracking results and better statistics in the bioshield. However, the computational speed is 260 times slower due to the involved long histories.

A program has been developed to tune the ADVANTG WW mesh in order to mitigate the long history problem. This python program is able to process the WW mesh, extract parts of the cells inside a container, and adjust the WW using several methods. Compared to the WW mesh without tuning, the computational speed is 37 times faster, and the statistics of the results are further improved.

In addition, the McDeLicious code has been extended to enable the simulation source neutrons generated with constant weight. It is concluded, however, that the use of a WW mesh together with the extended McDeLicious version does not show a clear improvement of the computational speed and statistical accuracy of the tracking results.

#### ACKNOWLEDGMENTS

This work has been carried out within the framework of the EUROfusion Consortium and has received funding from the Euratom research and training programme 2014-2018 under grant agreement No 633053. The views and opinions expressed herein do not necessarily reflect those of the European Commission.

#### REFERENCES

1. J. Knaster et al., The accomplishment of the Engineering Design Activities of IFMIF/EVEDA: The European–Japanese project towards a Li(d,xn) fusion relevant neutron source, Nuclear Fusion 55(8)(2015) 086003.
2. A. Ibarra et al., A stepped approach IFMIF/EVEDA towards IFMIF, Fusion Science and Technology, 66 (2014) 252–259.
3. X-5 Monte Carlo Team, MCNP – A General Monte Carlo N-Particle Transport Code Overview and Theory (Version 5, vol. I), Los Alamos National Laboratory,

Report LA-UR-03-1987 (Revised 10/3/05), (24 April 2003).

4. S. W. Mosher, A. M. Bevill, S. R. Johnson, et al. ADVANTG—An Automated Variance Reduction Parameter Generator[J]. ORNL/TM-2013/416, Oak Ridge National Laboratory, 2013.
5. S. P. Simakov, U. Fischer, K. Kondo and P. Pereslavysev, Status of the McDeLicious Approach for the D-Li Neutron Source Term Modeling in IFMIF Neutronics Calculations, Fusion Sci. Technol., 62 (2012), 233-239.
6. FENDL-3.1b, <http://www-nds.iaea.org/fendl>.
7. PyNE - The Nuclear Engineering Toolkit, <http://pyne.io>.